NUMERICAL STUDY OF MULTIPHASE FLOWS IN A LADLE FOR DIFFERENT CLOSURE MODELS

*Eshwar Kumar Ramasetti, Ville-Valtteri Visuri, Petri Sulasalmi, Aki Kärnä and Timo Fabritius

Process Metallurgy Research Unit, University of Oulu
PO Box 4300, 90014 University of Oulu, Finland
*eshwar.ramasetti@oulu.fi

ABSTRACT

Computational Fluid Dynamics (CFD) modelling is increasingly being used for studying various metallurgical processes. In secondary steelmaking, gas stirring is used in ladles to enhance the mixing of the steel. This work aims at numerical study to investigate the effect of different closure models on of the flow analysis in a two-phase gas-stirred ladle. The study represents a cylindrical geometry, in which liquid Wood's metal represents the liquid metal phase and nitrogen gas is injected through nozzle located centrically or eccentrically at the bottom of the vessel. Three-dimensional CFD simulations were carried out using the commercial software package ANSYS FLUENT using Euler-Euler multi-phase model. To study the influence of turbulence models on the accuracy of the CFD analysis, three different models Standard *k*-ε, *k*-ω and Reynolds Stress Model (RSM) were employed. Furthermore, four different gas flow rates (100, 200, 500 and 800 cm^3/s) were used for studying the effect of gas flow rates on the flow velocities. The simulation results were compared with the available experimental data of the liquid velocity profiles, volume fraction of gas and turbulent kinetic energy at different heights in the ladle. The RSM model showed a good accuracy of results when compared to experimental results, but it requires more computational time when compared to other turbulence models. The simulation results using the liquid Wood's metal/nitrogen system were compared to water/air and liquid steel/argon systems to check the effect of material properties on the flow velocities in the ladle. The results provide useful guidelines for numerical modelling of fluid flows in steelmaking ladles and suggest that the RSM turbulence model is better suited for studying gas injection in metallurgical ladles than *k*-ε or *k*-ω models.

Keywords: Steelmaking, Computational Fluid Dynamics (CFD), Secondary Metallurgy, Multi-phase flows, Euler-Euler model, Turbulence Modelling.

INTRODUCTION

In secondary metallurgy of steelmaking, gas stirring is a very common practice to improve the homogenization of the metal bath composition, temperature, desulphurization, and removal of inclusions. To study this phenomena various physical and mathematical modelling approaches have been developed.

Mazumdar et al. (1) have developed a physical and mathematical model to investigate the gas injection operations in steel making ladles. The investigations included the bubble rise velocity, and the variation of liquid rise velocity as a function of gas flow rate, and these were compared to experimental measurements. The role of turbulence models was assessed by Mazumdar and Guthrie (2) in predicting the flow fields generated in a 150-ton steel ladle with and without tapered side walls. A mathematical model describing turbulent re-circulatory flows and alloy dispersion in a ladle was presented by Mazumdar and Guthrie (3).

Schwarz et al. (4) used the standard *k*-*ε* turbulence model to investigate the void fraction and flow velocities in a two-phase gas stirred ladle. These simulation results were in good agreement with the data published by Mazumdar and Guthrie (2). A mathematical model which describes the fluid flow in a bubble stirred ladle is presented by Johansen et al. (5). Their model predicts the mean velocities, bubble dispersion, turbulent characteristics and gas-liquid interaction, and the simulations results of these investigations showed a satisfactory agreement with the experimental results.

To describe two-phase flow phenomena in a gas-stirred system for steel making Lou et al. (6) studied the influence of turbulent dispersion force, drag and lift forces on the liquid flow velocity, gas fraction and turbulent kinetic energy. The mathematical model developed was based on the Euler-Euler approach and the simulation results were compared to experimental results. Mendez et al. (7) performed a numerical simulation to study the effects of non-drag forces (virtual mass, lift and turbulent dispersion forces) on the gas fraction and liquid flow velocities in the ladle. A Eulerian model approach was used by Turkoglu et al. (8) to investigate the liquid flow velocity, gas fraction and temperature fields in a cylindrical ladle through bottom air injection. The turbulence in the liquid phase was modeled by a two-equation *k*-*ε* turbulence model and the numerical results were compared to the experimental measurements available in the literature.

Davidson et al. (9) conducted numerical simulations to investigate the magnitude of bubble rise velocity, center line void fraction and the central plume in a liquid bath where gas is injected from the bottom. The numerical simulation results were compared to the experimental measurements conducted by Castillejos and Brimacombe (10).

Domgin et al. (11) carried out a detailed experimental and numerical work to investigate the mean velocity distribution and turbulent kinetic energy in cylindrical steel bath where gas is injected through the bottom. The numerical simulations were based on Euler-Euler and Euler-Lagrange approaches and computational results based on Euler-Euler approaches were in good agreement with the experimental ones measured.

A study of two different turbulence modelling approaches (*k-ε* and RSM) was conducted by Park et al. (12) for a gas stirred ladle system. The investigations included the flow velocities, gas fraction and turbulent kinetic energies. The results showed that the turbulent kinetic energies predicted by *k-ε* turbulence model were higher and that the RSM and *k*-ε model are not suitable for predicting highly swirling flows.

Experiments and numerical simulations were carried out by Szekely et al. (13) for a water model of an argon-stirred ladle system. The simulation was performed by solving the turbulent Navier-Stokes equations and were based on using Spalding's *k-ω* turbulent model. The results showed good predictions of flow velocity and gas fractions when compared to the experimental measurements. A similar kind of work was also done by Ilegbusi et al. (14) investigating the flow velocities in a water model of an argon gas-stirred ladle through experiments and simulations. The simulation results were compared for two different turbulent models (*k*-ε and anisotropic eddy viscosity model). The predicted simulation results of mean velocity and turbulent parameters were compared to the experimental measurements.

Xie and Oeters (15) carried out experimental measurements for the flow velocity in a ladle with liquid Wood's metal with nitrogen gas injected through centric blowing. The liquid flow was measured using magnetic probes for various blowing conditions. The measurements for bubble behavior, as well as the local gas fraction and the rising velocity of bubbles were measured by Xie et al. (15) for different gas flow rates and nozzle diameters. The results were presented in the form of axial and radial velocities, gas volume fraction and for the turbulent kinetic energy at different heights of the ladle. Xia et al. (16) carried out numerical simulations and validated the experimental measurements axial and radial velocity profiles of Xie and Oeters (15) and Xie et al. (17) for different drag forces and lift coefficients. On the other hand, there was no detailed description of effect of different turbulence modelling approaches for the flow velocity in the ladle. Therefore, it is necessary to validate the experimental measurements with numerical simulations for different turbulence models.

The primary objective of the current work is to develop a mathematical model based on a Euler-Euler approach for a two-phase gas stirred ladle. This model would be able to simulate the flow in the ladle with Wood's metal as the liquid phase and nitrogen gas blown from the nozzle. These results are compared to the experiments of Xie and Oeters (15) and Xie et al. (17). Furthermore, this mathematical model would be able to study the effect of different modelling liquids phases (liquid Wood's metal, liquid steel and water) properties on the flow in the ladle.

MATHEMATICAL MODEL

The mathematical model is identical to the ladle used by Xie and Oeters (1992) and Xie et al. (1992) for experimental measurements. The ladle model is 400 mm in diameter and the height is 370 mm, filled with liquid Wood's metal/liquid steel/water with nitrogen/argon/air injected through a nozzle with a diameter of 3 mm located centrally/eccentrically at the bottom, as shown in Figure 1 below. Four different flow rates 100, 200, 500, 800 cm^3/s are used to study the effect of the flow rates on the flow velocities.

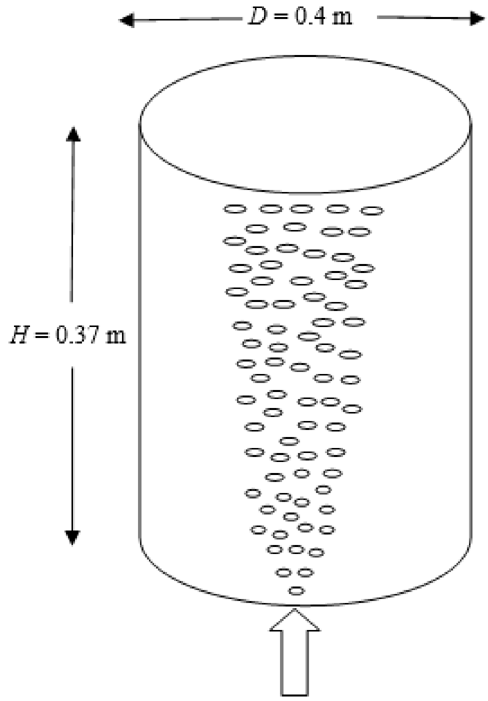

Figure 1: Schematic of ladle model.

The Euler-Euler multi-phase model

In the present work, Eulerian-Eulerian two-phase model is used. This model gives information about the volume fraction for every phase at a certain point in flows with multiple phases by providing a description of each phase and by explaining the probability of that phase being present at that point. Between the two phases there is some force of attraction and it is included through the drag force, lift force and virtual mass effect (defined as the net force between phases per unit volume).

The governing equations for the Eulerian-Eulerian two-phase model are described below (18)

Continuity equation:

$$\frac{\partial}{\partial t}\left(\alpha_{\mathrm{g}}\rho_{\mathrm{g}}\right) + \nabla.\left(\alpha_{\mathrm{g}}\rho_{\mathrm{g}}\overrightarrow{u_{\mathrm{g}}}\right)$$

$$= \sum_{l=1, l\neq g}^{n} \dot{m}_{lg} - \dot{m}_{gl} \quad (1)$$

Momentum equation:

$$\frac{\partial}{\partial t}\left(\alpha_g \rho_g \vec{\rho}_g\right) + \nabla.\left(\alpha_g \rho_g \vec{u_g}\,\vec{u_g}\right) = -\alpha_g \nabla_l + \nabla.\,\bar{\bar{\tau}}_g + \alpha_g \vec{g} + \vec{F_g} + \sum_{l=1, l\neq g}^{n} \dot{m}_{lg}\,\vec{v}_{lg} - \dot{m}_{gl}\,\vec{v}_{gl} + \sum_{P=1, P\neq k}^{n} \vec{R_{lg}} + \vec{F_{lift}} + \vec{F_{vm}}, \quad (2)$$

where

$$\bar{\bar{\tau}}_g = \alpha_g \mu_g \left(\nabla \vec{u_g} + \nabla \vec{u_g^{T}}\right) + \alpha_g \left(\lambda_g - \frac{2}{3}\mu_g\right)\left(\mu_g \bar{\bar{I}}\right) \quad (3)$$

In Equation (3), $\vec{R_{lg}}$ symbolizes the drag force between the phases 'l' and 'g'. The mathematical description of the drag force is written below:

$$\vec{R_{lg}} = K_{lg}(\vec{u_l} - \vec{u_g}), \quad (4)$$

where

$$K_{lg} = \frac{3}{4}\,\alpha_l\,\alpha_l\,\mu_g\,\frac{Re\,C_d}{d_l^2}. \quad (5)$$

In the above equation (5), K_{lg} is the coefficient of the drag exchange momentum and C_d is the drag coefficient between the phases. In equation (2), F_{lift} denotes the lift force acting on the secondary phase 'g' due to primary phase 'l' and the term $\vec{F_{vm}}$ symbolizes the virtual mass force. In the present work, the lift force and virtual mass terms are neglected.

Turbulence models

The three different turbulence models used in the current work are described below.

a. *The k* - ε model

The k-ε model is the most widely used and accepted turbulence model in present day industry and research. From the equations of this model it is possible to calculate both the values of turbulent kinetic energy with the first transport variable 'k' and the turbulent dissipation rate with the second transport variable 'ε'. The governing equations for this model are written below. (18)

$$\frac{Dk}{Dt} = \frac{\partial}{\partial x_j}\left(\frac{v_t}{\sigma_k}\frac{\partial k}{\partial x_j}\right) + P_k - \varepsilon, \quad (8)$$

$$\frac{D\varepsilon}{Dt} = \frac{\partial}{\partial x_i}\left(\frac{v_t}{\sigma_k}\frac{\partial \varepsilon}{\partial x_j}\right) + C_{\varepsilon_1}\frac{\varepsilon}{k}P_k - C_{\varepsilon_2}\frac{\varepsilon^2}{k}, \quad (9)$$

where

$$P_k = -\bar{u}_i\,\bar{u}_j\,\frac{\partial u_i}{\partial u_j}. \quad (10)$$

b. *The k* - ω model

The k-ω turbulence model is also a two-equation model similar to the k-ε model. The second transport variable 'ω' in this case determines the specific dissipation, whereas the first variable 'k' determines the kinetic energy of turbulence. The governing equations are written below. (18)

$$\frac{Dk}{Dt} = \frac{\partial}{\partial x_j}\left(\left(\mu + \frac{k}{\omega}\right)\frac{\partial k}{\partial x_j}\right) + P_k - \beta\omega k, \quad (11)$$

$$\frac{D\omega}{Dt} = \frac{\partial}{\partial x_j}\left(\left(\mu + \sigma_w\frac{k}{\omega}\right)\frac{\partial w}{\partial x_i}\right) + \frac{\sigma_d}{\omega}\frac{\partial k}{\partial x_j}\frac{\partial \omega}{\partial x_j} + \frac{P_k\,\gamma\omega}{k} - \beta\omega^2, \quad (12)$$

where

$$P_k = \tau_{ij}\frac{\partial u_i}{\partial x_j}, \quad (13)$$

$$v_t = \frac{k}{\omega}. \quad (14)$$

c. The Reynolds Stress Model (RSM)

Reynolds stress model is a five-equation turbulence model, and is has a relatively lesser computational cost than Large Eddy Simulations and Direct Numerical Simulations. The Reynolds stress transport equation is written below. (18)

$$\frac{DR_{ij}}{Dt} = D_{ij} + P_{ij} + \pi_{ij} + \Omega_{ij} - \varepsilon_{ij}, \quad (15)$$

where D_{ij} is the diffusion term, P_{ij} is the production term, π_{ij} is the slow-pressure correlation term, ε_{ij} is the dissipation term and Ω_{ij} is the rotational term, respectively. The descriptions of P_{ij}, π_{ij} and ε_{ij} are provided in Eqs. 16, 17 and 18 respectively.

$$P_{ij} = -\left(R_{im}\frac{\partial U_j}{\partial x_m} + R_{jm}\frac{\partial U_i}{\partial x_m}\right), \quad (16)$$

$$\pi_{ij} = -C_1\frac{\varepsilon}{k}\left(R_{ij} - \frac{2}{3}k\,\delta_{ij}\right) - C_2\left(P_{ij} - \frac{2}{3}P\,\delta_{ij}\right), \quad (17)$$

$$\varepsilon_{ij} = \frac{2}{3} \epsilon \, \delta_{ij}, \quad (18)$$

where ε is dissipation rate of turbulent kinetic energy and δ_{ij} is the Kronecker delta. The diffusion term is expressed as follows:

$$D_{ij} = \frac{\partial}{\partial x_m} \left(\frac{v_t}{\sigma_k} \frac{\partial R_{ij}}{\partial x_m} \right), \quad (19)$$

where $v_t = C_\mu \frac{k^2}{\varepsilon}$, $\sigma_k = 1.0$ and $C_\mu = 0.9$. The rotational term is described by:

$$\Omega_{ij} = -2\, \omega_k \left(R_{jm}\, e_{ikm} + R_{im}\, e_{jkm} \right), \quad (20)$$

where ω_k is the rotation vector,

$e_{ijk} = 1$, if i, j , k are in cyclic order,
$e_{ijk} = -1$, if i, j , k are in anti-cyclic order, and
$e_{ijk} = 0$, if any two indices are same.

The Schiller-Naumann drag model

The Schiller-Naumann drag model (19) is derived from Stokes' law. According to the Stokes' law, the drag coefficient C_{D} for the flow past spherical particles can be calculated according to

$$C_{\mathrm{D}} = \frac{24}{\mathrm{Re}}, \quad (21)$$

where Re is the Reynolds number. The Stokes' law is valid for Re << 1. The expression shown in Eq. 21 has been modified to suit high Reynolds numbers by including inertia. The modified mathematical expression is written below:

$$C_{\mathrm{D}} = \frac{24}{\mathrm{Re}} \left(1 + \frac{3}{16} \mathrm{Re} \right), \quad (22)$$

It has been shown that the above expression deviates from the experimental results at high Reynolds numbers. It was re-modified for Re<800 by Schiller and Naumann (19), and it can be written as follows:

$$C_{\mathrm{D}} = \frac{24}{\mathrm{Re}} \left(1 + 0.15\, \mathrm{Re}^{0.687} \right). \quad (23)$$

In the present work, the Schiller-Naumann drag model has been used to exchange momentum between the two phases (liquid Wood's metal and nitrogen gas).

Boundary conditions

Along the cylindrical walls of the ladle, a no-slip boundary condition is assumed as is the pressure outlet condition at the top free surface of the ladle. For the nozzle injection, a constant gas velocity inlet boundary condition is assumed. At the beginning of the calculation, the volume fraction of liquid (liquid wood's metal/liquid steel/water) is set to unity and the volume fraction of gas (nitrogen/argon/air) is set to zero.

Material properties

In the current work, Wood's metal, an alloy with a low melting point, was employed as the liquid phase, while nitrogen gas was injected through the nozzle in most of the calculations. The results of the Wood's metal/nitrogen system are compared with liquid steel/argon and water/air systems to check the effect of modelling liquid properties on the flow velocities in the ladle.

Table 1: Comparison of physical properties of liquids

Liquid	Density (kg/m^3)	Dynamic Viscosity (Pa·s)
Wood's metal	9400	0.0042
Steel	7000	0.0044– 0.0062
Water	1000	0.001

Numerical Procedures

The numerical simulations were carried out in the ANSYS FLUENT 17.0 software and were based on a Euler-Euler multiphase model. The standard *k*-ε, *k*-ω and RSM turbulence models describe the turbulence in the continuous fluid. The interaction between the two phases is defined by the Schiller-Naumann drag force and no lift force was applied. The diameter of a bubble was assumed as 3 mm for all of the cases. The convergence criteria was set to $10^{-5}$and all unsteady simulations were carried out on a physical time scale of 0.001 s per time step. All simulations were stopped once the flow became steady and the total time was 30 s.

The hybrid mesh for the cylindrical ladle was generated in ICEM CFD software. Trial calculations were conducted to study the mesh independency using three different meshes with sizes 132775, 249265 and 404187 cells. It was found all the three meshes produced similar results and the mesh with 249265 elements was then used for all the simulations.

RESULTS AND DISCUSSSION

Euler-Euler simulations were carried out for the ladle model with liquid Wood's metal and nitrogen gas injected through a nozzle located at the bottom. To study the effect of gas flow rates on the liquid flow velocities in the ladle model, four different velocities (100, 200, 500 and 800 cm^3/s) were employed (RSM turbulence model is used). Figure 2 shows the increase in the range of liquid flow velocities in the ladle with increases in the gas flow rate. The simulation results for liquid velocity profiles at four different heights in the ladle for three different turbulence models (*k*-ε, *k-ω* and Reynolds Stress Model) along with the measured data from Xie and Oeters (1992) are shown in Figure 3. As seen in Figure 3, the simulation results using *k*-ε and *k-ω* turbulence models follow the same liquid velocity profile for the measured data but the velocities are very high at all heights. On the other hand, the results of the liquid velocity profiles using RSM exhibit good agreement with the experimental data at heights 0.05 m and 0.15 m from the bottom. At heights of 0.25 m and 0.35 m, the RSM model predicts slightly higher velocities when compared to the experimental data but lower than *k*-ε and *k*-ω turbulence models.

The simulation results of gas volume fraction in the ladle at four different heights for three turbulence models are shown in Figure 4. It can be seen that numerical simulation results using *k*-ε and *k*-*ω* turbulence models show a high peak in gas volume fraction at all four heights in the ladle. The numerical predictions using the RSM model also show high peaks in gas volume fractions at all the heights and do not match the experimental measurements. However, these predictions give low peaks in gas volume fractions when compared to the other two turbulence models. The results would have been better for *k*-ε and *k*-*ω* turbulence models if we could have tested different parameter values instead of using the default values from the Ansys Fluent software.

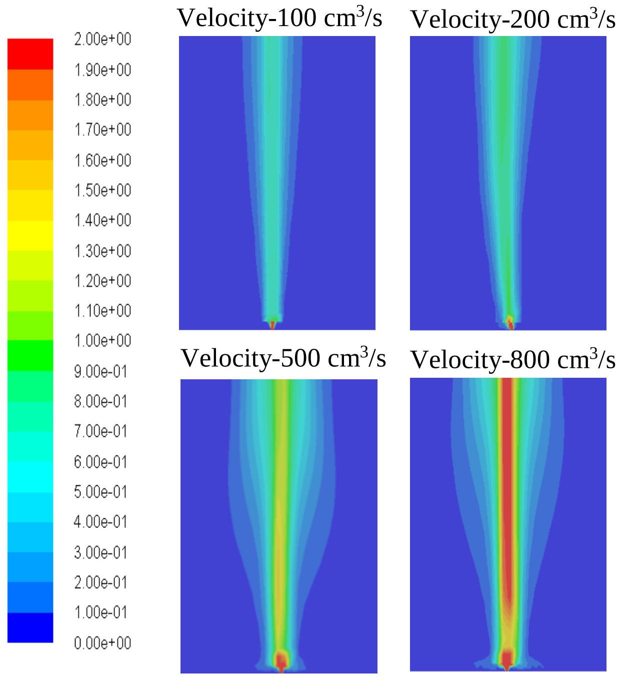

Figure 2: Velocity field distribution for different gas flow rates

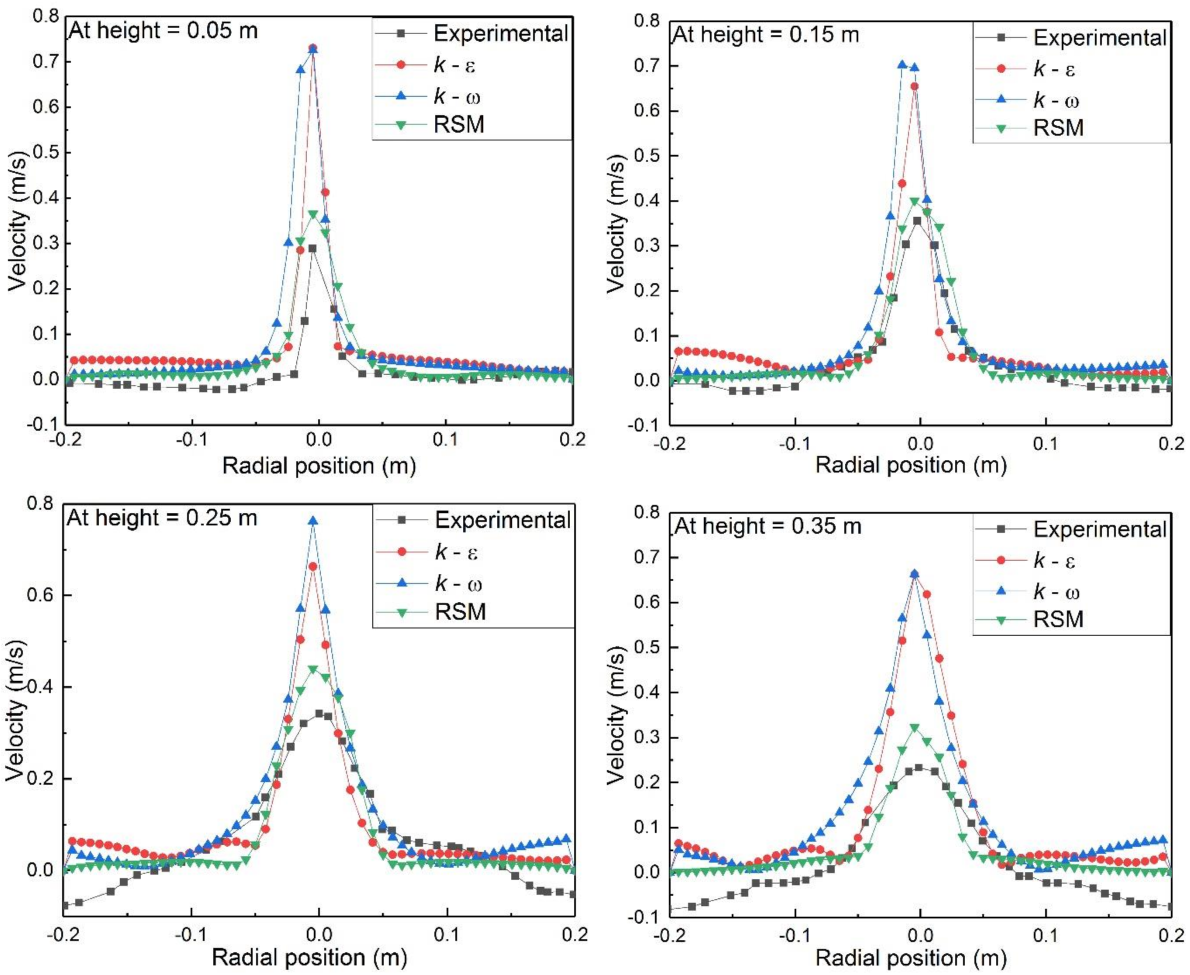

Figure 3: Comparison of liquid flow velocity profiles at different heights in the ladle for different turbulence models to the experimental data from Xie and Oeters (1992).

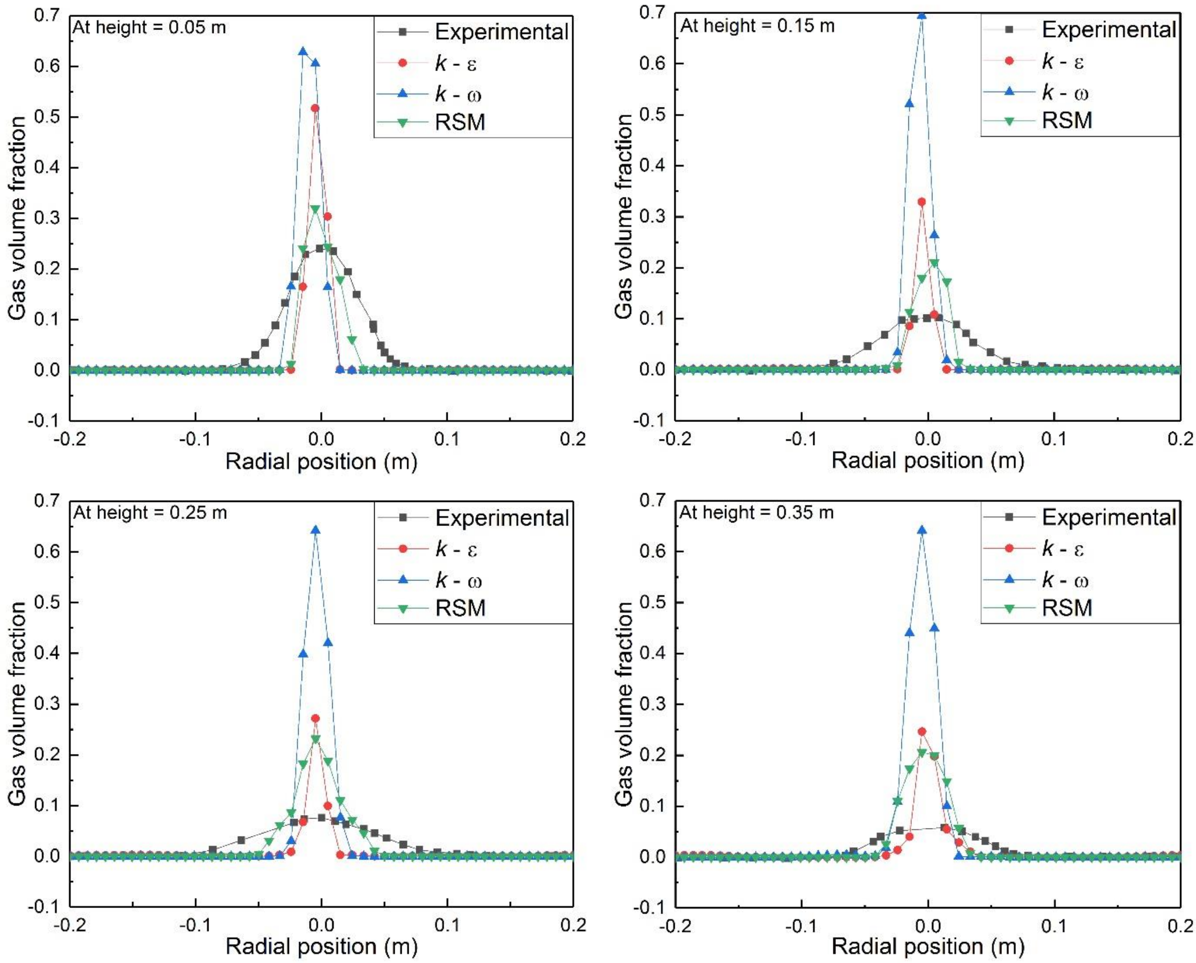

Figure 4: Comparison of Gas fraction distribution profiles at different heights in the ladle for three different turbulent models to the experimental data from Xie et al. (1992).

Figure 5 depicts the velocity distribution in the ladle for a gas flow rate of 200 cm^3/s when the gas is injected through a nozzle located at a centric and eccentric position using the RSM turbulence model. As seen from Figure 5, when the nozzle is located near the wall, a strong attraction of the flow by the wall is observed. Thus, it appears that the wall has a great influence on the flow distribution in the ladle. Figure 6 shows the comparison of numerical predictions of turbulent kinetic energy for a gas flow rate of 800 cm^3/s with the experimental measurements by Xie and Oeters (15). As seen from Figure 6, the simulations results for turbulent kinetic energy follow the same trend and agree reasonably well with the experimental measurements at heights of 0.05 m, 0.15 m and 0.25 m. However, the agreement is poor at a height of 0.35 m.

Figure 7 shows the comparison of velocity profiles at a height of 0.35m for three different domains (liquid wood's/nitrogen, liquid steel/argon and water liquid/air) with experimental data from Xie and Oeters (15). As seen in Figure 7, the velocity profiles of liquid Wood's metal/nitrogen and liquid steel/argon domains are almost similar. This is because of the density and viscosity of the liquid Wood's metal are more similar to liquid steel than to those of water and mercury. The numerical predictions follow the same trends of the experimental measurements by Xie and Oeters (15) and Xie et al. (17) but do not match them quantitatively.

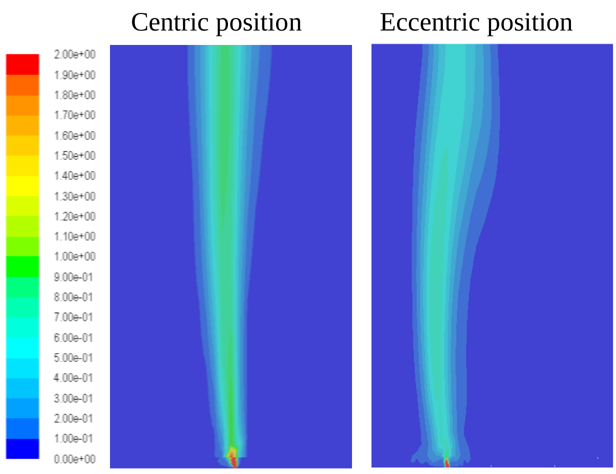

Figure 5: Comparison of velocity distribution profiles for a gas flow rate of 200 cm^3/s when the nozzle is located in centric and eccentric positions at the bottom of the ladle.

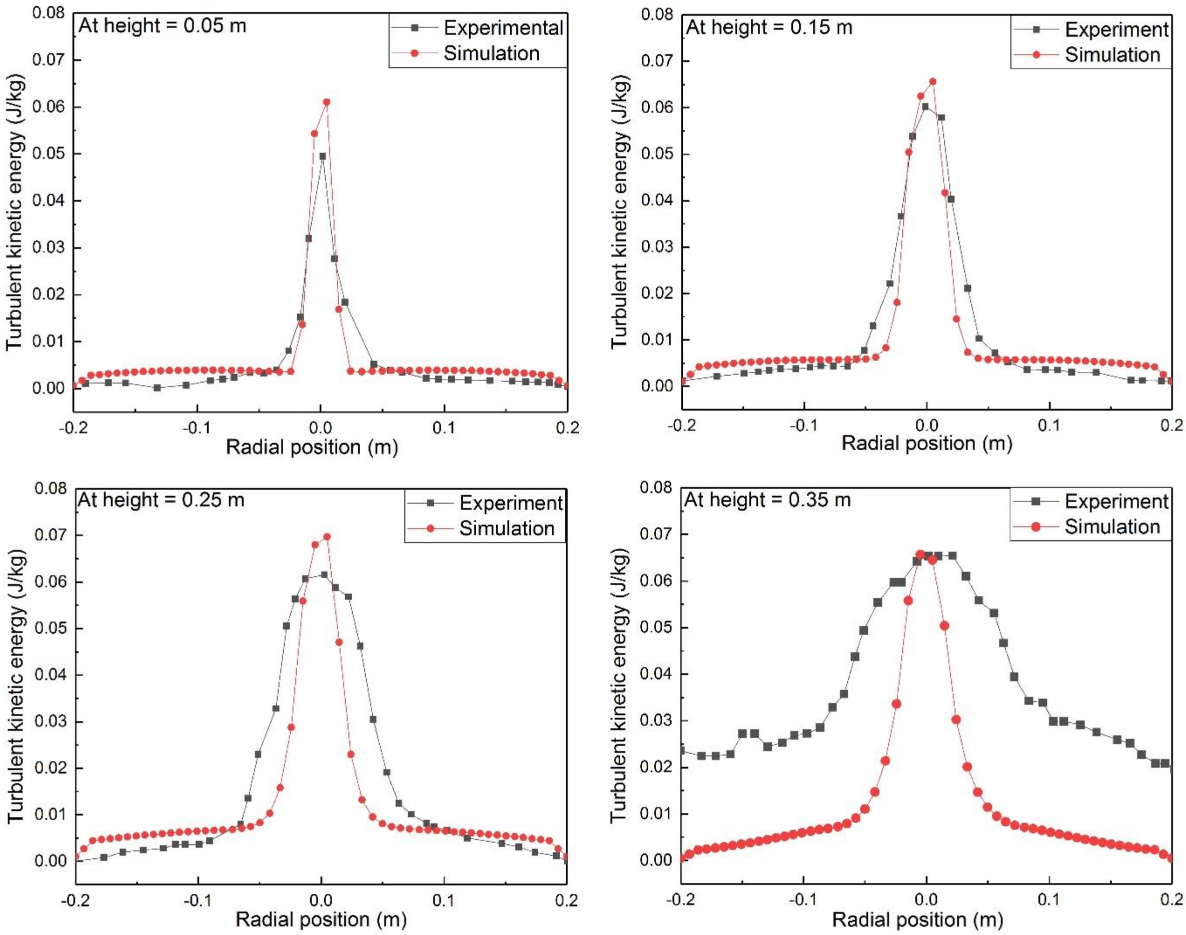

Figure 6: Comparison of turbulent kinetic energy profiles for a gas flow rate of 800 cm^3/s to experimental data (Xie and Oeters 1992a) at four different heights in the ladle.

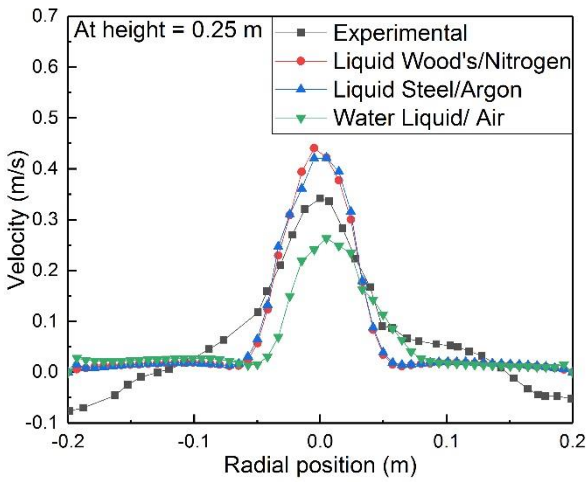

Figure 7: Comparison of velocity profiles at height 0.25m for different domains to experimental data from Xie and Oeters (1992).

CONCLUSIONS

Computational Fluid Dynamics simulations were performed for two phase flows in a ladle with liquid Wood's metal/liquid steel/water liquid agitated by nitrogen/argon/air gas injection. These simulations were carried out for four different gas flow rates (100, 200, 500 and 800 cm^3/s) to study the effect of gas flow rates on the flow velocities in the ladle. A detailed comparison was made for simulation results of the liquid flow velocity, volume fraction of gas and turbulent kinetic energy at different heights in the ladle with the experimental measurements from Xie and Oeters (15) and Xie et al. (17). Among the different turbulence modelling approaches (k-ε, k-ω and RSM), the RSM model had decently accurate results when compared to experimental results. The results suggest that the RSM model is preferable in modelling two phase flows in a gas-stirred ladle, but it requires more computational time when compared to k-ε and k-ω turbulence modelling approaches.

To check the effect of material properties on the flow velocities in the ladle, the simulation results using liquid Wood's metal/nitrogen system were compared to liquid steel/argon and water liquid /air systems. The present results provide information on CFD in modelling two phases in steelmaking ladles.

ACKOWLEDGMENT

The research work was financially supported by the European Union under Marie Sklodowska-Curie Horizon 2020 project, which is gratefully acknowledged.

NOMENCLATURE

ρ density, kg/m^3
Re Reynolds number
C_d drag coefficient
C_l lift coefficient
n constant in breakage model
d diameter of phase considered
α_g volume fraction of gas phase
α_l volume fraction of liquid phase
ρ_l density of liquid phase
ρ_g density of gas phase
λ_g shear viscosity for gas phase
υ_t turbulent kinematic viscosity
σ_k turbulent Prandtl number
ε dissipation rate of turbulence kinetic energy
σ surface tension
μ_g bulk velocity for gas phase

Subscripts
l liquid phase
g gas phase

REFERENCES

(1) Mazumdar, D. and Guthrie, R.I.L. (1995): "The Physical and Mathematical Modelling of Gas Stirred Ladle Systems". *ISIJ International,* Vol. 35, pp. 1–20.
(2) Mazumdar, D. and Guthrie, R.I.L. (1985): "Numerical computation of flow and mixing in ladle metallurgy steel making operations". *Applied Mathematical Modelling,* Vol. 10, pp. 25–32.
(3) Mazumdar, D. and Guthrie, R.I.L. (1985): "Hydrodynamic modeling of some gas injection procedures in ladle metallurgy operations". *Metallurgical Transactions B,* Vol. 16, pp. 83–90.
(4) Schwarz, M.P. and Turner, W.J. (1987): "Applicability of the standard *k*-ε turbulence model to gas stirred baths". *Applied Mathematical Modelling,* Vol. 12, pp. 273–279.
(5) Johansen, S.T. and Boysan, F. (1988): "Fluid dynamics in bubble stirred ladles: Part 2 Mathematical Modelling". *Metallurgical Transactions B,* Vol. 19. pp. 755–764.
(6) Lou, W. and Miaoyong Zhu, M. (2013): "Numerical Simulation of Gas and Liquid Two-Phase Flow in Gas-Stirred Systems Based on the Euler–Euler Approach". *The Minerals, Metals and Material Society,* Vol. 44, pp. 1251–1263.
(7) Mendez, C.G., Nigro, N. and Cardona, A. (2004): "Drag and non-drag influences in numerical simulations of metallurgical ladles". *Journal of Materials Processing Technology,* Vol. 160, pp. 296–305.
(8) Turkoglu, H. and Farouk, B. (1990): "Numerical computations of fluid flow and heat transfer in a gas-stirred liquid bath". *Metallurgical and Materials Transactions B,* Vol. 21, pp. 771–781.
(9) Davidson, M.R. (1999): "Numerical calculations of two-phase flow in a liquid bath with bottom gas-injection: The central plume". *Applied Mathematical Modelling,* Vol. 14, pp. 67–76.
(10) Castillejos, A.H. and Brimacombe, J. K. (1986): "Structure of turbulent gas-liquid plumes in vertically injected jets". *Proceedings of the Fourth International Conference on Injection Metallurgy, Luleå, Sweden*.
(11) Domgin, J.F., Gardin, P. and Brunet, M. (1999): "Experimental and numerical investigations of gas stirred ladles". *Proceedings of the Second International Conference on CFD in the Minerals and Process Industries, Melbourne, Australia.*
(12) Park, H.-J. and Yang, W.-J. (2007): "Turbulent two-phase mixing in gas-stirred systems for continuous casting applications". *Numerical Heat Transfer Applications,* Vol. 31, pp. 493–515.
(13) Szekely, J., Wang, H.J. and Kiser, K.M. (1975): Flow pattern velocity and turbulence energy measurements and predictions in a water model of an argon stirred ladle". *Metallurgical Transactions B,* Vol. 7. pp. 287–295.
(14) Ilegbusi, O.J., Szekely, J., Iguchi, M., Takeuchi, H., Morita, Z.-I. (1993): A Comparison of Experimentally Measured and Theoretically Calculated Velocity Fields in a Water Model of an Argon Stirred Ladle". *ISIJ International,* Vol. 33, pp. 474–478.
(15) Xie, Y. and Oeters, F. (1992): "Experimental studies on the flow velocity of molten steels in a ladle at centric gas blowing". *Steel Research,* Vol. 63, pp. 93–104.
(16) Xia, J.L., Ahokainen, T. and Holappa, L. (1999): "Modelling of Flows in a Ladle with Gas Stirred Liquid Wood's Metal". *Proceedings of the Second International Conference on CFD in the Minerals and Process Industries, Melbourne, Australia.*
(17) Xie, Y., Orsten, S. and Oeters, F. (1992): "Behavior of Bubbles at Gas Blowing into Liquid Wood's metal". *ISIJ International,* Vol. 32. pp. 66-75.
(18) Schiller, L. and Naumann, A. (1935): "A drag coefficient correlation". Zeitschrift des Vereines Deutscher Ingenieure, Vol. 77. pp. 318–320.
(19) Ansys Fluent (2009), User's Guide, Canonsburg, PA, USA, Ansys, Inc